

A simulation study of energy transport in the Hamiltonian XY-model

Luca Delniy, Stefano Lepri^y and Roberto Liviz

^y Istituto Nazionale di Ottica Applicata and
Istituto dei Sistemi Complessi, Consiglio Nazionale delle Ricerche, Sezione
Territoriale di Firenze, largo E. Fermi 6 I-50125 Firenze, Italy
^z Dipartimento di Fisica, Università di Firenze, Sezione INFN, Unità INFN and
CSDC Firenze, via G. Sansone 1 I-50019, Sesto Fiorentino, Italy

Abstract. The transport properties of the planar rotator model on a square lattice are analyzed by means of microcanonical and non-equilibrium simulations. Well below the Kosterlitz-Thouless-Berezinskii transition temperature, both approaches consistently indicate that the energy current autocorrelation displays a long-time tail decaying as t^{-1} . This yields a thermal conductivity coefficient which diverges logarithmically with the lattice size. Conversely, conductivity is found to be finite in the high-temperature disordered phase. Simulations close to the transition temperature are instead limited by slow convergence that is presumably due to the slow kinetics of vortex pairs.

Key word: Transport processes / heat transfer (Theory)

Submitted to: Journal of Statistical Mechanics: theory and experiment

PACS numbers: 63.10.+a 05.60.-k 44.10.+i

1. Introduction

Physical phenomena in reduced spatial dimension ($d = 1; 2$) are often qualitatively different from their three-dimensional counterparts. The overwhelming role of statistical fluctuations and the presence of constraints in the motion of excitations can lead to peculiar effects like the impossibility of long-range order. In the context of non-equilibrium statistical mechanics, the existence of long-time tails in fluids [1] leads to ill-defined transport coefficients, thus implying a breakdown of the phenomenological constitutive laws of hydrodynamics [2].

A remarkable example is the anomalous behavior of heat conductivity for $d = 2$. This issue attracted a renewed interest within the statistical-mechanics community after the discovery that the thermal conductivity of anharmonic chains diverge in the thermodynamic limit [3]. Since then, those anomalies have been detected in a series of different models. An exhaustive account is given in Ref. [4], where the effects of lattice dimensionality, disorder and external fields for the validity of Fourier's law are discussed in detail. The signature of anomalous behavior is a non-integrable algebraic decay of the correlator of the heat current J (the Green-Kubo integrand) at large times

$$\langle J(t) J(0) \rangle / t^{1-\alpha}; \quad t \rightarrow +\infty \quad (1)$$

where $0 < \alpha < 1$ and $\langle \cdot \rangle$ is the equilibrium average. For a finite system of linear size L this implies that the finite-size conductivity $\kappa(L)$ diverges in the $L \rightarrow \infty$ limit. In fact, in the framework of linear-response theory, κ can be estimated by cutting off the integral in the Green-Kubo formula at the transit time L/v (v being some propagation velocity of energy carriers). Taking into account Eq. (1) one straightforwardly obtains $\kappa \sim L^\alpha$.

Simulation studies of specific models [4] as well as analytic arguments [5], lead to the surmise that anomalous conductivity should occur generically whenever momentum is conserved. Moreover, the exponent α should be largely independent on the microscopic details as suggested by a renormalization-group calculation of Ref. [5] that predicts $\alpha = (2-d)/(2+d)$. For $d = 1$ the resulting value $\alpha = 1/3$ is roughly close to the numerical estimates although some substantial deviations have been observed in specific cases [7, 6, 8]. The situation is even more controversial $d = 2$ where the predicted t^{-1} decay yields a logarithmic singularity which is consistent with simulation data [9], while other works report significant deviations and dimensional crossovers [10].

When extending the analysis to the 2d case, one naturally wonders how the possibility of observing critical phases may affect the anomalous energy conduction. The first example one may think of is of course the Ising model. It has however been shown that, at least for a specific choice of the spin dynamics, the latter displays a normal conductivity at all temperatures [11]. In a more general perspective, this is consistent with the idea the breakdown of momentum conservation removes transport anomalies. Indeed, the field-theoretic counterpart of the Ising model, the so called ϕ^4 theory, acquires an on-site non-linear interaction that breaks translational invariance. Although we are not aware of any study of this model in the ordered phase, it is known

that the lattice ϕ -model in the high-temperature phase displays a finite conductivity in the thermodynamic limit [12].

In this present paper, we present a simulation study of the transport properties of a model of rotators coupled on a square lattice, akin to the celebrated XY-model (see e.g. [13] and references therein for a comprehensive review). As it is well known, the latter is characterized by the presence of the so called Kosterlitz-Thouless-Berezinskii (KTB) phase transition at finite temperature between a disordered high-temperature phase and a low-temperature one, where vortices condense.

As recalled above, the fact the momentum (actually the angular momentum) is a constant of motion, makes this model a candidate for observing anomalous behavior. On the other hand, its 1d version is the only known exception to this requirement and displays normal transport, due to the presence of "dynamical defects" in the form of localized rotations that act as scattering centers for the heat carriers [14]. On the basis of this observation it is extremely interesting to investigate if and how the vortices play a similar role in the 2d case.

Before entering the details of the present work, it is important to mention that some evidence of the role of the vortex unbinding on the transport properties of the (modified) XY-model have been reported in Ref. [15]. Nonetheless, those results are mainly qualitative and we are thus motivated to undertake a more detailed analysis.

The paper is organized as follows. In section 2 we introduce the model and its microcanonical simulation. In Section 3 we recall the technique we used to investigate the non-equilibrium stationary state. The outcomes of numerical simulations for the disordered and critical phases are reported in Sections 4 and 5, respectively. Finally, we summarize and discuss our results in Section 6.

2. Hamiltonian dynamics of the XY-model

The XY or planar rotator model consists of a set of classical "spins" S_r of unit length confined in a plane, whose orientation is specified by the angle θ_r , with $r = (i; j)$ being an integer vector labelling the sites of a square lattice of size $N = N_x \times N_y$. It is known that this model does not admit equations of motion and therefore its canonical dynamics is usually simulated either by Monte-Carlo methods [16, 17] or by Langevin type equations [18, 19]. Microcanonical approaches consist instead, either in considering a three component spin model [20] or into adding a kinetic energy term [21]. The latter method, which we follow in the present work, can be also generalized to other physical systems (see e.g. the application to lattice gauge theories [22]). All these different dynamics should display the same static properties, as it has been verified up to some extent [21, 23]. We thus consider the Hamiltonian

$$H = \sum_r \frac{p_r^2}{2} + \sum_{\langle r, r' \rangle} [1 - \cos(\theta_r - \theta_{r'})]; \quad (2)$$

where $p_r = -\hbar \hat{p}_r$ is the angular momentum of the rotator. The sum ranges over the four nearest neighbors of site r , namely $r^0 = r + \hat{x}$ and $r^0 = r + \hat{y}$ where \hat{x} and \hat{y} are the unit vectors parallel to the lattice axis. It could be shown that (2) is obtained as the classical limit of a quantum Heisenberg Hamiltonian with an anisotropy term $\sum_r (S_r^z)^2$, using the representation introduced in Ref. [24]. We have set both the inertia of the rotators and the ferromagnetic coupling constant to unity so that the only physical control parameter is the energy per spin $e = H/N$. Actually, there is a second constant of the motion, the total angular momentum $P = \sum_r p_r$, whose choice affects the results in a trivial way. In the numerical simulations we set $P = 0$ to avoid global ballistic rotation.

A previous study of the static properties of (2) [23] showed that the system undergoes a KTB transition [13] at $e = e_{\text{KTB}} \approx 1.0$, corresponding to a kinetic temperature $T_{\text{KTB}} \approx 0.89$, which is in agreement with the value 0.894(5) obtained in the canonical ensemble [17]. One of the most striking features of the XY model is the presence of strong finite-size effects [25], e.g. the existence of a sizable magnetization for large samples, despite the fact that long-range order cannot occur for the infinite system. This has also some consequence on the dynamical correlation of the finite-size magnetization [26].

In the framework of linear-response theory, heat transport properties can be analyzed by computing the autocorrelation function (or, equivalently, the power spectrum) of the total heat current vector J at equilibrium. We thus need a microscopic expression that can be worked out by the procedure followed for other similar models [4]. In brief, it amounts to writing down a discretized continuity equation and, by means of the equation of motion, identify the proper expression of the local flux in terms of the canonical variables $(r; p_r)$. For model (2), $J = (J^x; J^y)$ can be written as a sum over all lattice sites

$$J^x = \frac{1}{2} \sum_r \sin(\theta_{r+\hat{x}} - \theta_r) \frac{\hbar}{\tau_{r+\hat{x}} + \tau_r} \quad (3)$$

$$J^y = \frac{1}{2} \sum_r \sin(\theta_{r+\hat{y}} - \theta_r) \frac{\hbar}{\tau_{r+\hat{y}} + \tau_r} \quad (4)$$

This latter expression is the correct one in the microcanonical ensemble with $P = 0$. Incidentally, notice that a suitable counterterm should be subtracted out if one wishes to work in a different statistical ensemble [27].

The numerical integration of the equations of motion (with periodic boundary conditions) is performed using the fourth-order McLachlan-Aela algorithm [28], which is an explicit scheme constructed from a suitable truncation of the evolution operator that preserves the Hamiltonian structure. One of the major merits of symplectic algorithms is that the error on the energy does not increase with the length of the run. The chosen time step (0.01-0.05 in our units) ensures that in every simulation energy fluctuates around the prescribed value with a relative accuracy below 10^{-5} .

As mentioned above, the main quantity of interest is the flux autocorrelation function $h_J(t) = J(0) \cdot J(t)$. For numerical purposes, we find more convenient to evaluate the power spectra $S(f)$, i.e. the squared modulus of the Fourier transform of each component

of J , averaged over a set of different initial conditions. These initial conditions were chosen by letting $\varphi_r = 0$ and drawing the $\varphi_r = 0$ at random from a Gaussian distribution with zero average and unit variance. The momenta are then all rescaled by a suitable factor to yield the desired value of the total energy. A transient is elapsed in order to start the averaging from a more generic phase{space point.

3. Non{equilibrium simulations

The non{equilibrium simulations have been performed by coupling all the rotators on the left and right edges of the lattice with two thermal baths operating at different temperatures T_+ and T_- . Periodic and fixed boundary conditions have been adopted in the direction perpendicular (y) and parallel (x) to the thermal gradient, respectively. Thermal baths have been simulated by applying the Nosé-Hoover method:

$$\begin{aligned} \ddot{\varphi}_r &= -\frac{\partial V}{\partial \varphi_r} - \tau_r [\dot{\varphi}_r^{+} - \dot{\varphi}_r^{-}] \\ \dot{\varphi}_r^{+} &= \frac{1}{2} \left(\frac{\partial}{\partial \varphi_r} \frac{\dot{\varphi}_r^2}{k_B T_+} \right) \quad 1A \\ \dot{\varphi}_r^{-} &= \frac{1}{2} \left(\frac{\partial}{\partial \varphi_r} \frac{\dot{\varphi}_r^2}{k_B T_-} \right) \quad 1A \end{aligned} \quad (5)$$

Here, V is the potential associated with (2), τ_r are the thermostat's response times, and δ_{ij} is the usual Kronecker symbol. Notice that each rotator is thermostatted independently and, accordingly, the Nosé-Hoover variables τ_r are vectors of length N_y . For computational purposes, simulations have been performed by fixing the aspect ratio $R = N_y/N_x < 1$. The choice of R results from a trade{off between minimizing the number of rotators (R small) and dealing with a genuinely 2d lattice ($R \rightarrow 1$). Indeed, too small values of R would require considering larger system sizes to clearly observe 2d features. For small lattices, we checked that the results are almost independent of the ratios employed hereby.

Since we are interested in the average values of the flux we have to check that the non{equilibrium stationary state is indeed attained. To this aim, we monitored that the average fluxes towards the boundaries

$$\begin{aligned} J^+ &= \frac{1}{N_x} \sum_j \dot{\varphi}_j^+ \frac{\partial}{\partial \varphi_j} \frac{\dot{\varphi}_j^2}{2} \\ J^- &= \frac{1}{N_x} \sum_j \dot{\varphi}_j^- \frac{\partial}{\partial \varphi_j} \frac{\dot{\varphi}_j^2}{2} \end{aligned} \quad (6)$$

were equal to the flux in the bulk, namely $\overline{J^+} = \overline{J^-}$ (the overline denotes a time average henceforth).

As observed before [4], the choice of the thermostat response times is crucial to the time needed to reach the stationary state, and to control the values of thermal resistance at the boundaries. In order to fasten the convergence, the initial conditions have been generated by thermostating each particle to yield a linear temperature profile

along the x direction. This method is very efficient, especially for large lattices, when thermalization within the bulk may be significantly slow.

Once the steady non-equilibrium state is attained, the relevant observables are accumulated and averaged in time. In particular we evaluated the local kinetic temperature $k_B T_x = \frac{2}{\tau}$ and the average energy fluxes $\overline{J^x}$ and $\overline{J^y}$, as defined by formulae (4), as well as the average fluxes towards the reservoirs \overline{J} . For obvious symmetry reasons, we expect (and indeed found) the $\overline{J^y}$ vanishes up to the statistical accuracy. Moreover, T_x depends only on the location along the x axis, and a further average is performed along y . Once the the average flux is computed, we evaluated the thermal conductivity coefficient from Fourier's law as

$$\kappa_x = \frac{\overline{J^x}}{j_x T j} , \quad \frac{\overline{J^x} N_x}{T_+ - T} \quad (7)$$

The last equality is only approximate, since the actual thermal gradient within the lattice is usually smaller than $(T_+ - T) = N_x$, due to boundary resistance effects [4]. In other words, the coefficient evaluated in this way should be regarded as an effective conductivity including both boundary and bulk scattering. As we are going to show in the next section the rescaled stationary temperature profiles, obtained for different values of N_x are such that the temperature gradient actually scales like N_x^{-1} . Therefore, definition (7) yields the same scaling behavior of the bulk conductivity.

4. The disordered phase

Let us start discussing the case of high energies or temperatures where the system is away from criticality. In the non-equilibrium simulations we fixed $T_+ = 1.5$ and $T_- = 1.4$ which are both well above the KTB transition temperature. Both response times of the Nose-Hoover thermostats have been set to the same value, $\tau = 1.0$. In fact, we have found empirically that such a choice minimizes boundary impedance effects, thus allowing for larger values of the heat flux. In order to improve the statistics, the temperature profiles and the measures of the heat flux have been averaged over 16 independent initial conditions. Numerical simulations have been performed by fixing the value of the aspect ratio to $R = 1/2$ and by increasing N_x up to 140. Some of the temperature profiles are reported in Fig. 1. They all exhibit a linear shape, which testifies to the expected temperature profile when Fourier's law holds. In Fig. 2 we show that the thermal conductivity, as defined by (7), is independent of N_x , with fluctuations around the average value, extending up to some 10 %.

These results have been compared with those obtained from equilibrium simulations. The value of the energy density has been chosen $e = 2$. Actually, this value corresponds approximately to the average temperature, $(T_+ + T_-)/2 = 2$, of the above mentioned non-equilibrium simulations. We want to point out that, for very large values of e , the kinetic energy dominates over the potential one and the system approaches the integrable limit of independent free rotators. Accordingly, in this limit the lattice is expected to behave as a perfect insulator, since the time scale for transmitting any

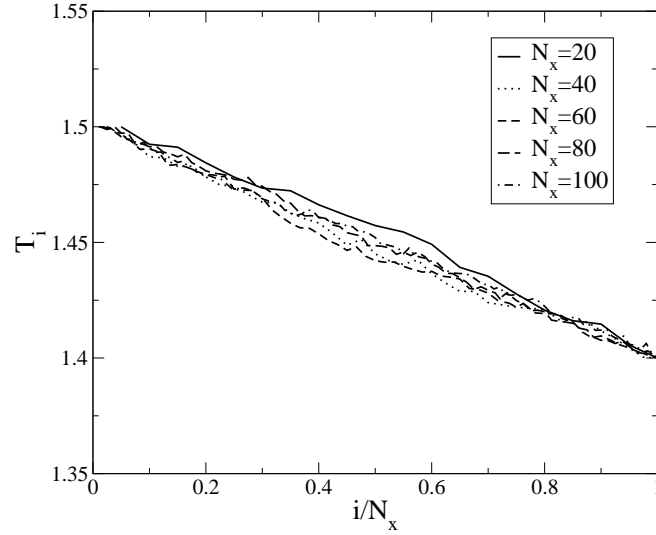


Figure 1. The temperature profile in the high-temperature phase for different values of N_x , which have been rescaled to the unit length. The response times of the Nose-Hoover thermostats are $\tau = 1.0$, which guarantee negligible boundary impedance effects.

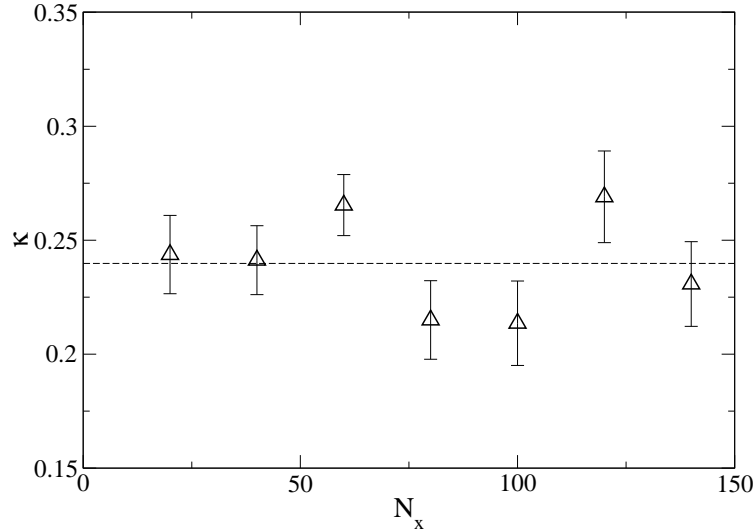


Figure 2. Finite-size conductivity in the disordered phase. Nose-Hoover thermostat with response times fixed to 1.0; Each point results from an average of 16 independent runs of about 10^6 time units each. The error bars are the error on the mean and the horizontal line is the average of all the measured values, $\kappa = 0.24$.

energy fluctuation diverges. In this respect, the choice $\epsilon = 2$ is appropriate, also because one can observe convergence of the quantities of interest over reasonable simulation times (typically, 10^6 time units). In Fig. 3 we show the heat flux spectra: they are independent of the lattice sizes and tend to a constant for small frequencies. This is a clear confirmation that no long-time tail is detectable and the thermal conductivity is a well-defined quantity in the thermodynamic limit. It should be remarked that the lineshape of these spectra cannot be fitted by a simple Lorentzian. This implies that in

the high-temperature phase the decay of time correlations cannot be reduced to a simple exponential law.

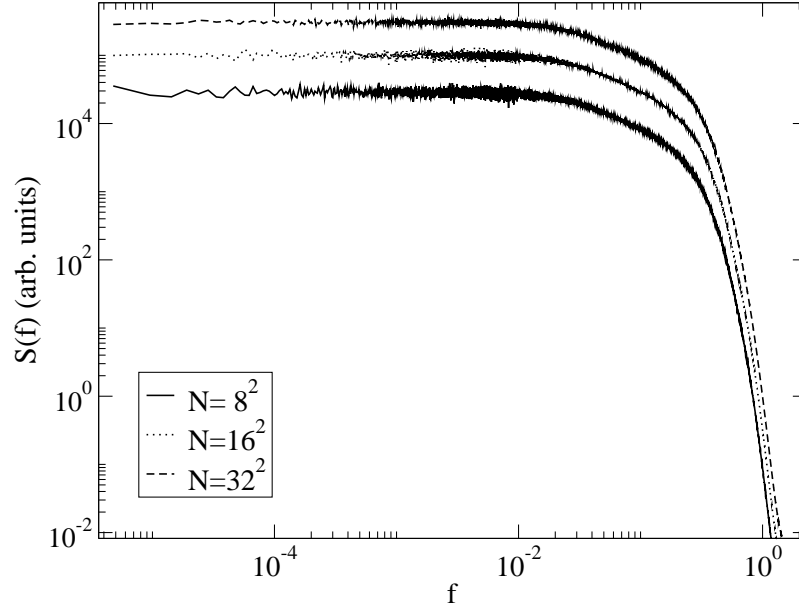


Figure 3. Power spectra of the heat current in the disordered phase for three different lattice sizes, $N = 8^2; 16^2; 32^2$. Data are averaged over 200 random initial conditions. In order to minimize statistical fluctuations, a further averaging of the data over contiguous frequency intervals has been performed. The three spectra actually almost overlap: this is why we have presented them after a vertical arbitrary shift in order to better distinguish one from each other.

5. The critical phase

A more interesting situation appears in the low-temperature phase. For what concerns the non-equilibrium calculations, we have fixed the thermostat's temperatures T to be well below the KTB transition value. At variance with the high-temperature phase, here the values of the response time of the Nose-Hoover thermostats have to be properly tuned in order to minimize boundary impedance effects. In particular, we have determined empirically the values $\tau_+ = 2.0$ and $\tau_- = 6.0$. Such different values, between themselves and also with respect to the high-temperature phase, indicate that fluctuations have to be slowed-down significantly in order to cope with the typical time scales of the dynamics. Moreover, we have performed the same statistical averaging as in the high-temperature case.

In Fig. 4 we show the temperature profiles obtained for $T_+ = 0.5; T_- = 0.4$ and different values of N_x . They exhibit a good data collapse when N_x is rescaled to the unit length. This confirms that also in the low-temperature phase the thermal gradient

scales like the inverse of the system size, $(T_+ - T_-)/N_x$. On the other hand, the temperature profile has assumed the typical non-linear shape, which testifies to anomalous thermal conductivity. Moreover, this shape is similar to the temperature profiles of the one and two-dimensional Fermi-Pasta-Ulam model [4].

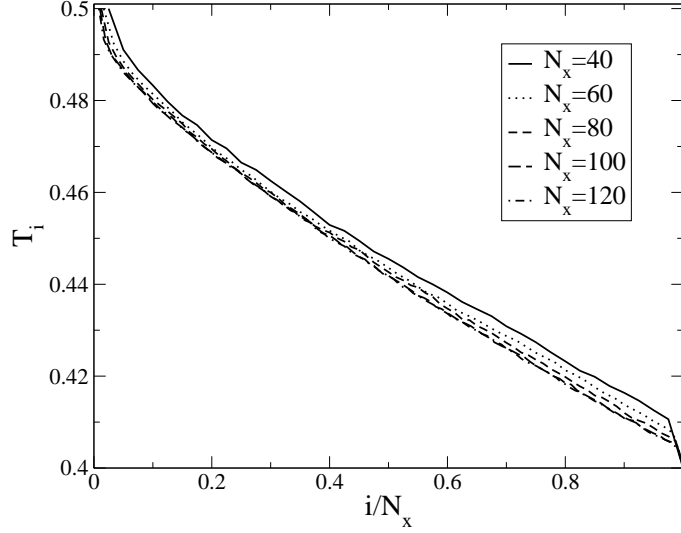


Figure 4. The temperature profile in the low-temperature phase for different values of N_x , which have been rescaled to the unit length. The response times of the Nose-Hoover thermostat are $\tau_+ = 250$ and $\tau_- = 650$, which minimize boundary impedance effects.

The finite-size thermal conductivity as a function of the longitudinal size N_x is reported in Fig. 5 for three different values of the boundary temperatures (with $T_+ - T_-$ kept fixed to 0.1). As expected, increasing T_- the conductivity decreases. More importantly, for fixed temperatures, the data all exhibit a systematic increase with N_x . In analogy with what found in the 2d Fermi-Pasta-Ulam model [9], the data for lower temperatures (curves (a) and (b)) can be well fitted by a logarithmic law

$$\kappa(N_x) = C_1 + C_2 \ln N_x : \quad (8)$$

Actually, a closer inspection of data set (c) reveals that the logarithmic fit is rather poor. In view also of the limited size range we have been able to explore, a convincing estimate of the growth law is unfeasible with the data at hand. This is presumably due to the fact that approaching T_{KT} requires longer times and sizes. In fact, we have observed that convergence of the averages considerably slows down in this region (about a factor 5 in passing from simulation (b) to (c)). The effect may be caused by slow thermalization of vortex pairs. Indeed, in this temperature region the vorticity starts to become sizeable [23] and a slower kinetics as well as relevant correction to scaling may thus be expected.

Following the analysis performed for the high-temperature phase, we have performed also microcanonical simulations, with periodic boundary conditions imposed in both lattice directions. We only considered the energy density $e = 0.5$ which roughly corresponds to $T = 0.45$.

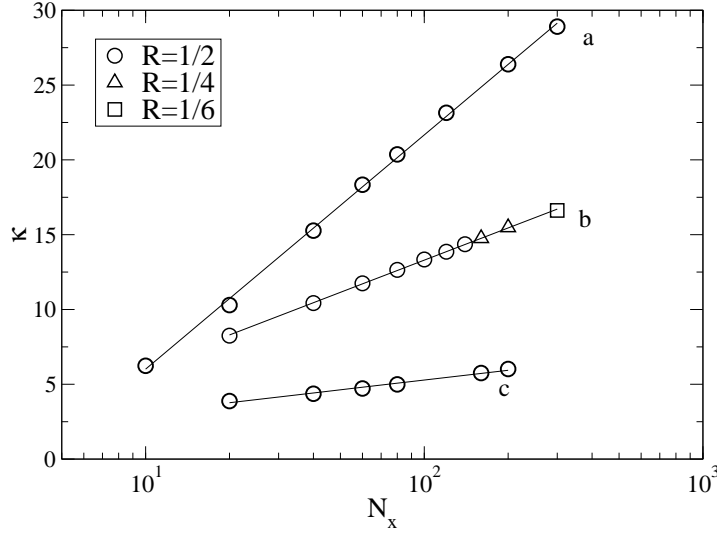


Figure 5. The thermal conductivity κ versus N_x in the low temperature phase for $T = 0.3; T_+ = 0.4$ (a), $T = 0.4; T_+ = 0.5$ (b) and $T = 0.6; T_+ = 0.7$ (c). Each point is the result of an average over 16 independent initial conditions, each one lasting for 10^6 time units. The error bars are of the order of the symbol's size. The solid lines are a best fit with a logarithmic law, Eq. (8).

In Fig. 6, we report the power spectra of the heat flux for different lattice sizes. For large frequencies ($f > f_c \approx 10^{-3}$) we have a f^{-2} behaviour which suggests a fast (exponential) decay of the correlation at short times. The crossover frequency f_c should be related to some typical time scale for the hydrodynamic effects to set in. In the low frequency limit, $f < f_c$, the data are consistent with a logarithmic singularity of the type (see the inset of Fig. 6)

$$S(f) = A + B \ln f \quad (9)$$

which, in turn, corresponds to a t^{-1} tail of the autocorrelation function. According to the argument exposed below Eq. (1), this would yield the logarithmic divergence (see Eq.(8)). Altogether, we conclude that the equilibrium and nonequilibrium approaches yield the same divergent behaviour.

It must be admitted that the fitting of the low frequency part with formula (9) is convincing only for the larger sizes. Actually, a power-law fit $S(f) / f^{0.4}$ is also compatible with the data obtained for smaller N values. On the other hand, this estimate cannot be taken seriously for a twofold reason. First of all, it may be easily attributed to finite-size effects. Moreover, it would imply a power-law divergent conductivity which, in turn, would be inconsistent with the nonequilibrium data (see again curve (b) in Fig. 5).

In view of the above fact, one may wonder why equilibrium simulations should be much more sensitive to finite-size effects than nonequilibrium ones. A reasonable

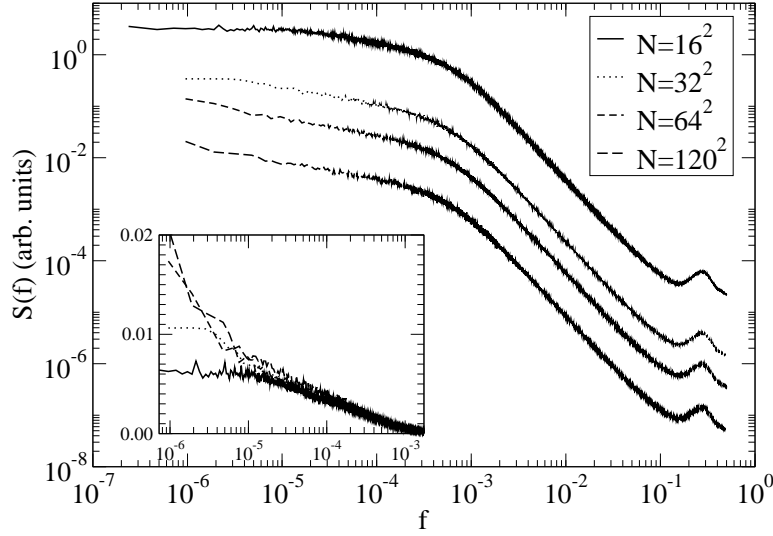


Figure 6. Power spectra of the heat current in the low temperature phase ($e = 0.5$), for four different lattice sizes $N = 16^2; 32^2; 64^2; 120^2$. Data are averaged over 400 random initial conditions. In order to minimize statistical fluctuations, a further averaging of the data over contiguous frequency intervals has been performed. The spectra are presented after a vertical arbitrary shift to better distinguish one from each other. The inset is an enlargement of the low frequency region in log{lin} scale.

qualitative explanation goes as follows. At low energies, where the isolated system is almost harmonic, it is very unlikely that a rotator turns from small oscillations to fast rotations. Moreover, for a small size system this process is even more unlikely as it demands a sufficiently large local energy fluctuation. Since this is the main scattering mechanism, one should wait for very long simulations before recovering the true asymptotic regime of energy transport. Conversely, in nonequilibrium simulations thermal baths act as external sources of fluctuations. These may favour the creation of the nonlinear excitations, thus shortening the time scale needed for the effects of the scattering process to be appreciated.

6. Concluding remarks

We have found numerical evidence that transport properties of the XY model on a finite lattice are drastically different in the high temperature and in the low temperature phases. In particular, thermal conductivity is finite in the former case, while in the latter it does not converge up to lattice sizes of order 10^4 . In the region where vorticity is negligible ($T < 0.5$) the available data suggest a logarithmic divergence with the system size analogous to the one observed for coupled oscillators [9]. Close to T_{KBT} , where a sizeable density of bounded vortex pairs are thermally excited, our data still suggest a divergence, whose law we cannot reliably estimate.

We want to point out that these results have been obtained consistently for

equilibrium and nonequilibrium simulations. The equivalence between these approaches is not granted a priori. On the other hand, this property has been verified for many other similar models [4], whose dynamics is of Hamiltonian type. In this respect, different choices of the dynamics (e.g. Monte Carlo) may not necessarily lead to the same conclusion.

This is a very important and interesting physical result: it indicates that in the low temperature phase some materials or states of matter, may behave as anomalously efficient heat conductors. For instance, as a direct consequence of the studies performed in this paper on the 2d XY model, liquid Helium films should be included in this class of materials. An experimental test confirming the prediction of the logarithmic divergence of the heat conductivity with the system size would be highly appropriate and welcome.

A complete hydrodynamic theory of the 2d XY model could certainly help in clarifying many of the aspects that our numerical approach cannot fully assess. For instance, an approach based on spin waves proved out to be effective in evaluating the dynamical correlations of the low temperature phase [29]. On the other hand, estimates of the energy-current correlators may be technically more difficult. Indeed, the heat flux is a constant to leading order and, accordingly, one has to account for higher order terms for the theory to make any sense. In this respect the calculations should be conceptually equivalent to estimating spin waves lifetimes [30]. It is not however clear how to include the effects of vortices and finite size magnetization in this framework. The hydrodynamics in the high temperature phase presumably should go through less technical troubles, although the construction of, say, a large deviation functional is far from trivial. Anyway, an effort in this direction is in our future agenda.

Acknowledgments

This work is supported by the INFN-PAIS project Transport phenomena in low-dimensional structures and is part of the PRIN 2003 project Order and chaos in nonlinear extended systems funded by MIUR-Italy. Part of the numerical simulation were performed at CINECA supercomputing facility through the INFN Iniziativa trasversale "Calcolo Parallelo" entitled Simulating energy transport in low-dimensional systems.

References

- [1] Poméau Y and Resibois R, 1975 Phys. Rep. 63 19
- [2] Kirkpatrick TR, Belitz D and Sengers JV, 2002 J. Stat. Phys. 109, 373
- [3] Lepri S, Livi R and Politi A, 1997 Phys. Rev. Lett. 78 1896
- [4] Lepri S, Livi R and Politi A, 2003 Phys. Rep. 377 1
- [5] Narayan O and Ramaswamy S, 2002 Phys. Rev. Lett. 89 200601
- [6] Lepri S, Livi R and Politi A, 2003 Phys. Rev. E 68 067102
- [7] Dhar A, 2001 Phys. Rev. Lett. 86 3554;
- [8] Casati G and Prosen T, 2003 Phys. Rev. E 67, 015203
- [9] Lippi A and Livi R, 2000 J. Stat. Phys. 100, 1147
- [10] Grassberger P and Yang L, unpublished [cond-mat/0204247]

- [11] Saito K, Takesue S and Miyashita S, 1999 Phys. Rev. E 59 2783
- [12] Hu B, Li B and Zhao H, 2000 Phys. Rev. E 61 3828; Aoki K and Kusnezov D, 2000 Phys. Lett. A 265 250
- [13] Gulacsi Z and Gulacsi M, 1998 Adv. Phys. 47 1
- [14] Giardinà C et al., 2000 Phys. Rev. Lett. 84 2144; Gendemann O V, and Savin A V, 2000 *ibid.* 84 2381
- [15] Dellago C and Posch H A, 1997 Physica A 237 95.
- [16] Tobochnik J and Chester G V, 1979 Phys. Rev. B 20 3761
- [17] Gupta R and Baille C F, 1992 Phys. Rev. B 45 2883
- [18] Loft R and DeGrand T A, 1987 Phys. Rev. B 35 1987
- [19] Jensen L M, Kim B J and Minnhagen P, 2000 Phys. Rev. B 61 15412
- [20] Evertz H G and Landau D P, 1996 Phys. Rev. B 54 12302
- [21] Kogut J and Polonyi J, 1986 Nucl. Phys. B [FS15] 265 313
- [22] Callaway D J E and Rahman A, 1982 Phys. Rev. Lett. 49 613
- [23] Leoncini X, Verga A D and Russo S, 1998 Phys. Rev. E 57 6377
- [24] J. Villain, 1974 J. Phys. (Paris) 35 27
- [25] Bramwell S T and Holdsworth P C W, 1993 J. Phys. Condens. Matter 5 L53
- [26] Lepri S and Russo S, 2001 Europhys. Lett. 55 512
- [27] Green M S, 1960 Phys. Rev. 119, 829
- [28] McLachlan P I and Atele P, 1992 Nonlinearity 5 541
- [29] Nelson D R and Fisher D S, 1977 Phys. Rev. B 16 4945
- [30] Wysin G M, Gouvea M E, and Pires A S T, 2000 Phys. Rev. B 62 11585

